Restriction of photoinduced electron transfer as a mechanism for aggregation-induced emission of trityl-functionalised maleimide fluorophore

Weijie Chi* and Ping-Ping Sun*

Department of Chemistry, School of Science, Hainan University, Haikou 570228, China

*Corresponding author E-mail: weijie_chi@hainanu.edu.cn (W. Chi)

E-mail:pingpingsun@hainanu.edu.cn (P. Sun)

List of Figure

Figure S1. The distributions of electron and hole of **BzMAM** in VES and AES, VES and AES denoted vertically excited state and adiabatic excited state, respectively. 2
Figure S2. The distributions of electron and hole of **Bz_2MAM** in VES and AES, VES and AES denoted vertically excited state and adiabatic excited state, respectively. 3
Figure S3. The distributions of electron and hole of **Bz_3MAM** in VES and AES, VES and AES denoted vertically excited state and adiabatic excited state, respectively. 3
Figure S4 Calculated relative electronic energies in the ground and excited states of Bz3MAM in water at M062X/TZVP level. 4
Figure S5. The difference in energies of low-lying excited state and ground state. 4
Figure S6. The distributions of HOMO and LUMO in **Bz_3MAM** in aggregates. 5
Figure S7. (a) the ONION model of dimeric Bz_3MAM in aggregate, (b) the excited-state potential energy surface in aggregate, (c) the distributions of HOMO and LUMO of Bz_3MAM based on the excited-state structure of dimer. 5
Figure S8. (a) optimized dimeric configuration of Bz3MAM, (b) isosurface maps of IRI for Bz3MAM-Dimer at M062X/TZVP level. 6
Figure S9.The diagram of complex structures BzMAM-MeOH, Bz_2MAM-MeOH, and Bz_3MAM-MeOH. 6
Figure S10. Two possible structures and relative energies of complexes in **Bz_3MAM-MeOH**. 7

$$RMSD = \sqrt{\frac{1}{N}\sum_{i}^{natom}[(x_i - x_i^{'})^2 + (y_i - y_i^{'})^2 + (z_i - z_i^{'})^2]} \quad \text{Equation 1}$$

where the x_i, y_i, *and* z_i, *denote the coordinates of the first molecule, and* $x_i^{'}$, $y_i^{'}$, *and* $z_i^{'}$ *represent the coordinates of the second molecule.*

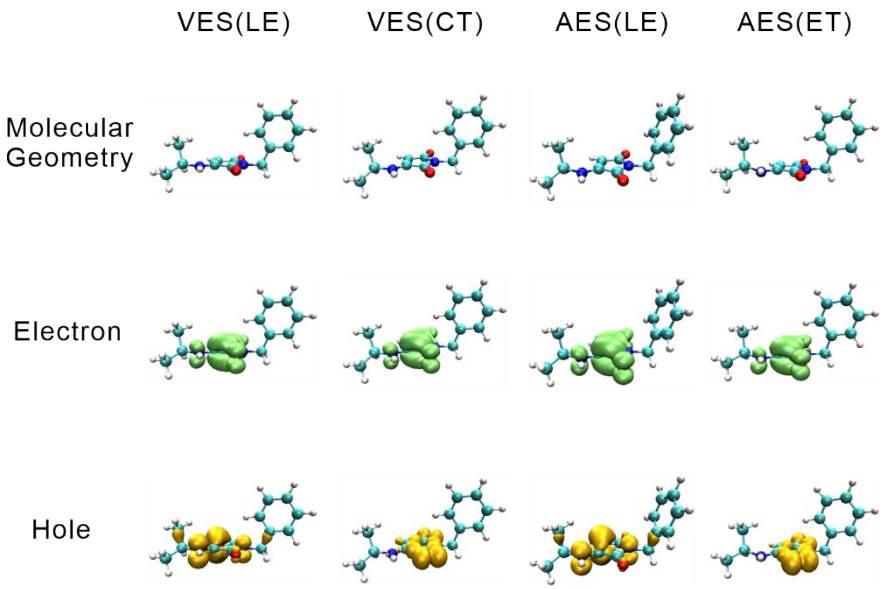

Figure S1. The distributions of electron and hole of **BzMAM** in VES and AES, VES and AES denoted vertically excited state and adiabatic excited state, respectively.

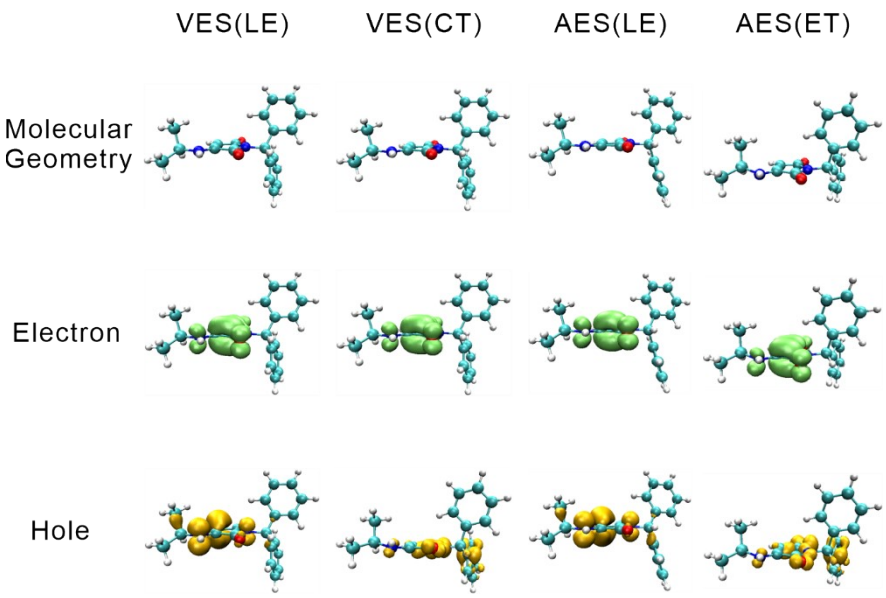

Figure S2. The distributions of electron and hole of **Bz_2MAM** in VES and AES, VES and AES denoted vertically excited state and adiabatic excited state, respectively.

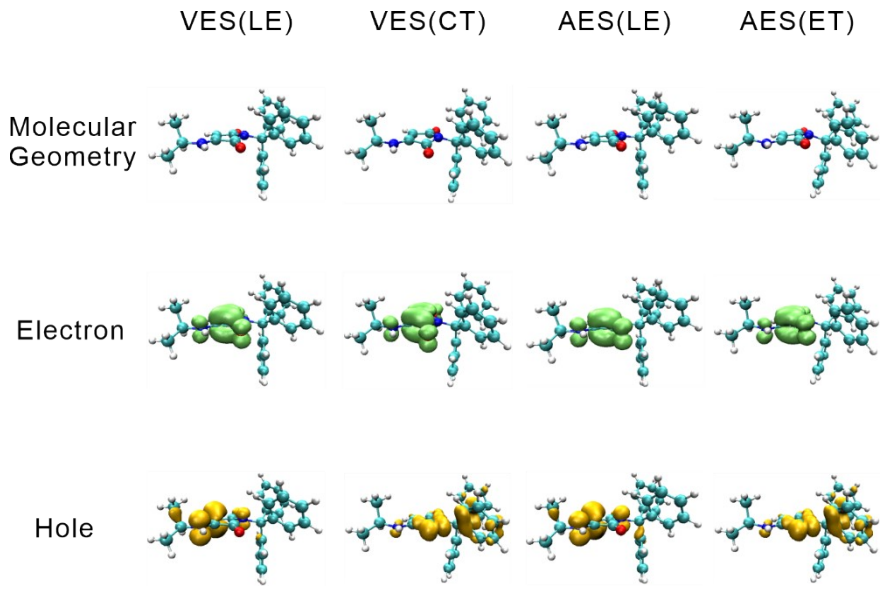

Figure S3. The distributions of electron and hole of **Bz_3MAM** in VES and AES, VES and AES denoted vertically excited state and adiabatic excited state, respectively.

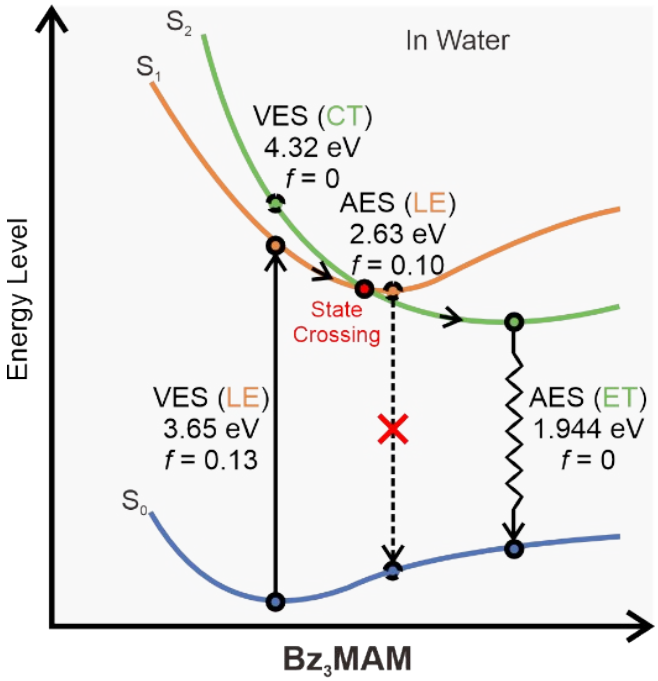

Figure S4 Calculated relative electronic energies in the ground and excited states of Bz3MAM in water at M062X/TZVP level.

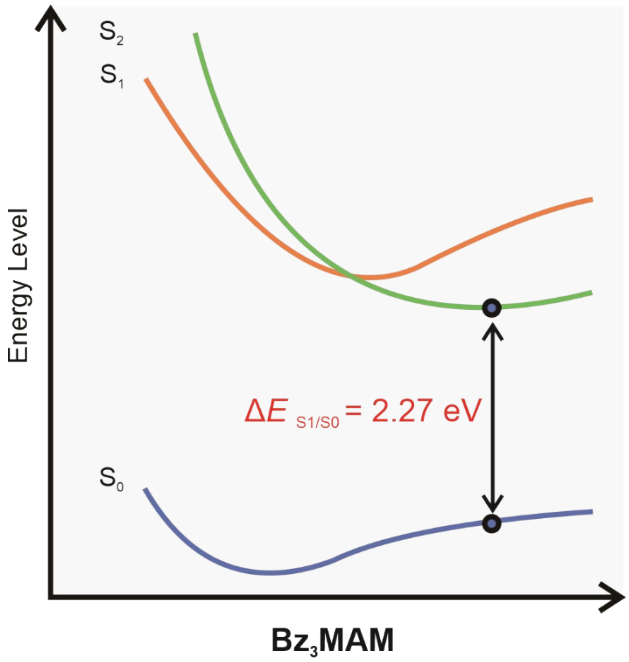

Figure S5. The difference in energies of low-lying excited state and ground state.

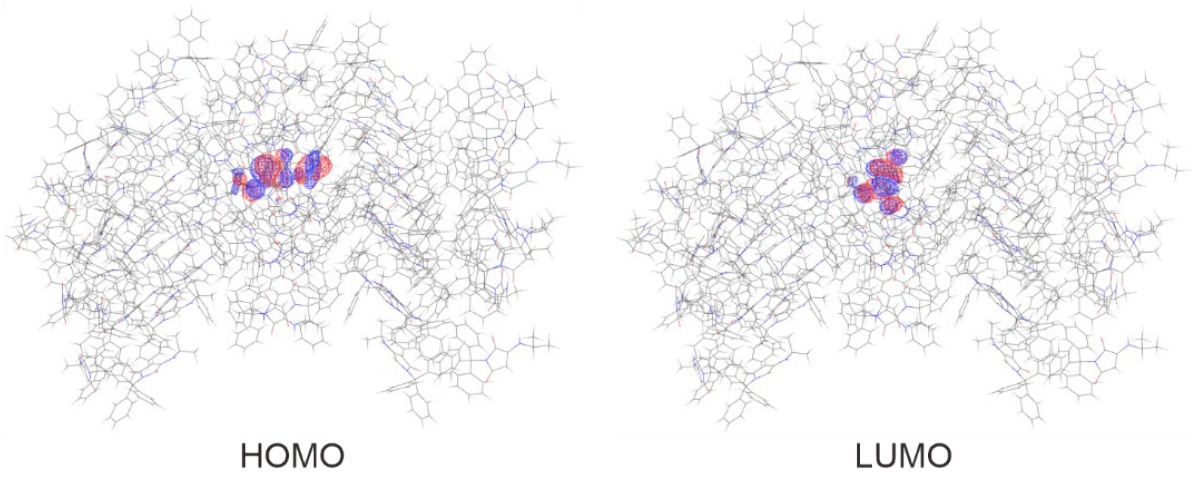

Figure S6. The distributions of HOMO and LUMO in **Bz_3MAM** in aggregates.

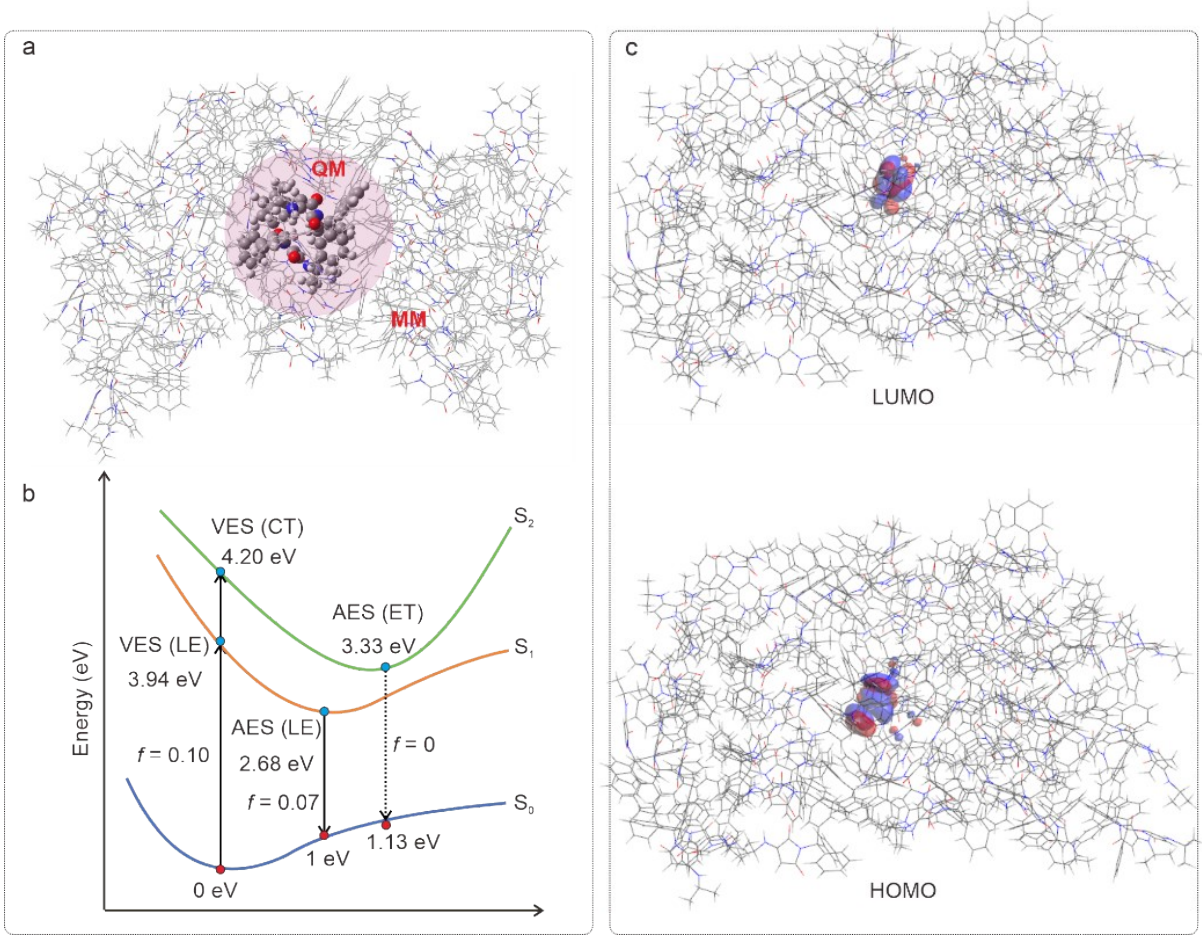

Figure S7. (a) the ONION model of dimeric Bz_3MAM in aggregate, (b) the excited-state potential energy surface in aggregate, (c) the distributions of HOMO and LUMO of Bz_3MAM based on the excited-state structure of dimer.

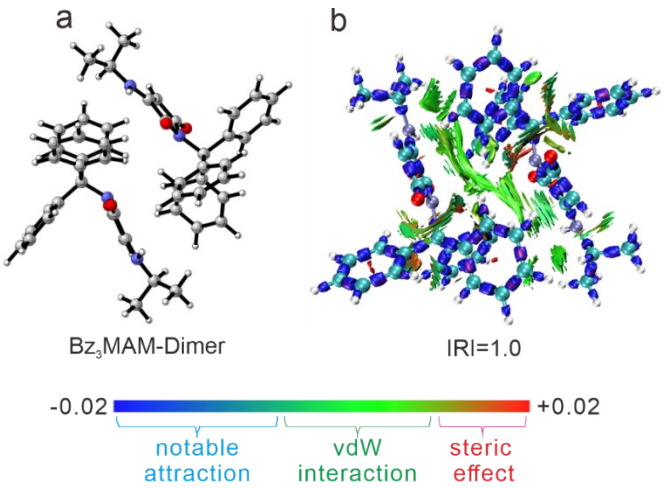

Figure S8. (a) optimized dimeric configuration of Bz_3MAM, (b) isosurface maps of interaction region indicator (IRI) for Bz_3MAM-Dimer at M062X/TZVP level, which was calculated using Multiwfn 3.7 code. The blue, green, and red denote the notable attraction, vdW interaction, and steric effect, respectively.

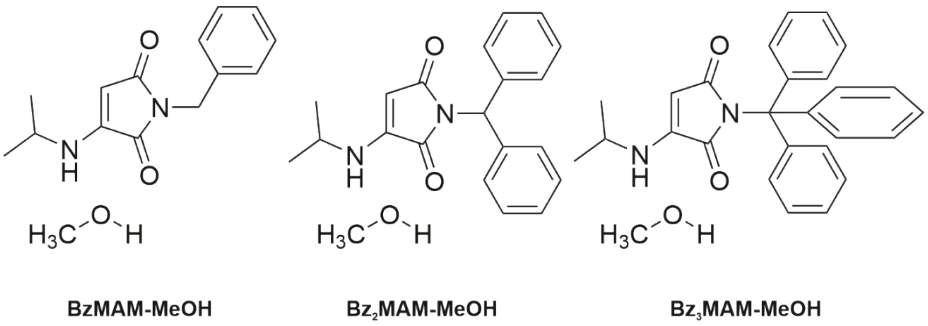

Figure S9.The diagram of complex structures BzMAM-MeOH, Bz_2MAM-MeOH, and Bz_3MAM-MeOH.

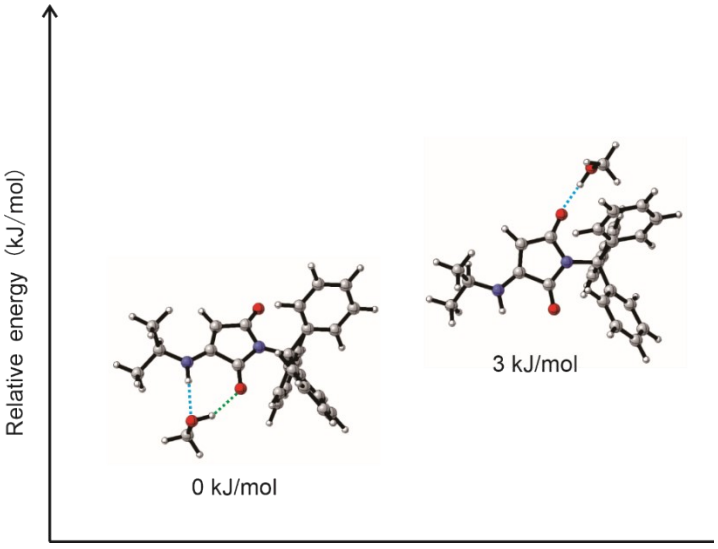

Figure S10. Two possible structures and relative energies of complexes in **Bz_3MAM-MeOH**.